Liquid Crystals
Publication details, including instructions for authors and subscription information:
http://www.informaworld.com/smpp/title~content=t713926090

Effect of the variation of swallow-tailed groups on the mesomorphic and electro-optical properties of chiral compounds derived from (<emph type="2">S</emph>)-2-(6-hydroxy-2-naphthyl)propionic acid

S. -L. Wu[a]; F. -C. Lu[a]
[a] Department of Chemical Engineering Tatung University 40 Chungshan N. Rd., 3rd Sec., Taipei, 104 Taiwan ROC,

Online publication date: 11 November 2010

To cite this Article Wu, S. -L. and Lu, F. -C.(2004) 'Effect of the variation of swallow-tailed groups on the mesomorphic and electro-optical properties of chiral compounds derived from (<emph type="2">S</emph>)-2-(6-hydroxy-2-naphthyl)propionic acid', Liquid Crystals, 31: 11, 1517 — 1523
To link to this Article: DOI: 10.1080/02678290412331304087
URL: http://dx.doi.org/10.1080/02678290412331304087

LIQUID CRYSTALS, VOL. 31, NO. 11, NOVEMBER 2004, 1517–1523

Effect of the variation of swallow-tailed groups on the mesomorphic and electro-optical properties of chiral compounds derived from (*S*)-2-(6-hydroxy-2-naphthyl)propionic acid

S.-L. WU* and F.-C. LU

Department of Chemical Engineering, Tatung University, 40 Chungshan N. Rd., 3rd Sec., Taipei, 104, Taiwan, ROC

Three homologous series of chiral swallow-tailed compounds, alkyl (*S*)-2-{6-[4-(4′-alkoxyphenyl)benzoyloxy]-2-naphthyl}propionates, (S)HNP(*p*,*n*,*q*) derived from (*S*)-2-(6-hydroxy-2-naphthyl)propionic acid in conjugation with a variety of swallow-tailed groups, attached to the external side of the chiral centre, have been synthesized and their mesomorphic and electro-optical properties studied. Both (S)HNP(*p*,1,2) and (S)HNP(*p*,1,3) exhibited an enantiotropic antiferroelectric SmC_A^* phase. This implys that the swallow-tailed groups in the molecules favour zigzag pairing of the molecules in the smectic phase. The maximum $\mathbf{P}_S$ values of compounds (S)HNP(*p*,1,2) in the antiferroelectric phase were measured in the range 21–30 nC cm^{-2}; those of compounds (S)HNP(*p*,1,3) were in the range 15–23 nC cm^{-2}, indicating that these chiral compounds possess low polarity. The electro-optical response of the compounds in the antiferroelectric SmC_A^* phase displayed thresholdless V-shaped switching.

1. Introduction

Our previous studies showed that the chiral swallow-tailed compounds series I, (S)HNP ($p=8$–12, $n=0$, $q=2$), as shown in the formula below, possess antiferroelectricity with thresholdless, V-shaped switching behaviour [1, 2]. This switching mode was first found in an antiferroelectric liquid crystal mixture and reported by Inui *et al.* [3]. Extended studies on the Inui mixture showed that the V-shaped switching behaviour strongly depends on the type of polyimide, thickness of the alignment layer, cell gap, and the type of cell [4–8]. Little, however, has been reported concerning the effect of molecular structure on the appearance of V-shaped switching.

In this work, therefore, we have designed three new series II, III and IV of chiral swallow-tailed compounds, (S)HNP(*p*,*n*,*q*), for the investigation of mesomorphic and electro-optical properties. They are structurally similar to series I, (S)HNP(*p*,0,2), with variation in the chiral swallow-tailed lengths, *n* and *q*. It is worth noting that achiral compounds with swallow-tailed terminal moieties have been demonstrated to possess a SmC_{alt} phase with antiferroelectric-like structure [9]. The general structural formulae of the three new chiral swallow-tailed compounds (S)HNP (*p*,*n*,*q*) are depicted below.

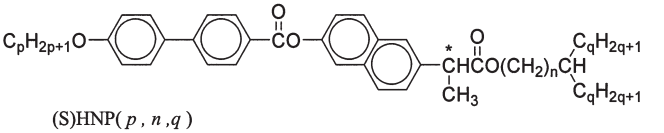

(S)HNP(*p*, *n*, *q*)

Ⅰ : (S)HNP(*p* = 8-12,0,2) Ⅱ : (S)HNP(*p* = 10-12,0,3)

Ⅲ : (S)HNP(*p* = 8-12,1,2) Ⅳ : (S)HNP(*p* = 9-14,0,3)

2. Experimental

2.1. *Characterization of materials*

The purity of the intermediate and final products was checked by thin layer chromatography and further confirmed by elemental analysis using a Perkin-Elmer 2400 spectrometer. The structures of the intermediate and final products were analysed by nuclear magnetic resonance spectroscopy using a Jeol EX-400 FTNMR (^{1}H NMR, 400 MHz) spectrometer.

Phase transition temperatures and corresponding phase transition enthalpies were determined by differential scanning calorimetry (DSC) using a Perkin-Elmer DSC7 calorimeter at a running rate of 5°C min^{-1}. Mesophases were identified principally with a Nikon Microphot-FXA optical microscope in conjunction with Mettler FP82-HT hot stage, using clean, untreated slides and coverslips. The antiferroelectricity of the materials was further characterized from switching behaviour, optical response and dielectric properties measured using parallel-aligned cells, purchased from

*Author for correspondence; e-mail: slwu@ttu.edu.tw

Liquid Crystals ISSN 0267-8292 print/ISSN 1366-5855 online © 2004 Taylor & Francis Ltd
http://www.tandf.co.uk/journals
DOI: 10.1080/02678290412331304087

Linkam Sci. Instr., Ltd. (5 μm) and E.H.C. Co., Japan (2 μm and 25 μm).

Spontaneous polarization ($\mathbf{P}_s$) was measured by a triangular wave method [10]. The temperature and frequency dependences of the real ε' and imaginary ε'' parts of the dielectric constant were investigated in the frequency range 20 Hz to 1 MHz. The measurement was made using a self-balancing Hewlett-Packard precision LCR meter (HP4284A) under computer control. The measuring electric field was chosen to be 1 $V_{P\text{-}P}$, to ensure linearity between the polarization and the oscillating field [11]. The temperature was controlled by a personal computer connected to a Mettler FP80 heat controller through an RS232 interface.

The optical response was measured using a He-Ne laser (5 mW, 632.8 nm) for the probe; the transmittance of the probe beam through the cell, between crossed polarizers whose axes were parallel and perpendicular to the smectic layer normal, was detected by a photodiode.

2.2. *Preparation of materials*

The starting chiral compound for the synthesis of the chiral liquid crystals was (*S*)-2-(6-methoxy-2-naphthyl)propionic acid, purchased from Tokyo Chemical Industry (TCI) Co. Ltd., Japan, with an optical purity greater than 99% enantiomeric excess. Tetrahydrofuran and dichloromethane were dried by treating with $LiAlH_4$ and CaH_2, respectively, and distilled before use.

The synthetic procedures were carried out in the same manner as described previously [12] and are shown in the scheme. The chiral moiety (*S*)-2-(6-methoxy-2-naphthyl)propionic acid, (S)MNP, was esterified with the appropriate alcohols in the presence of *N*, *N*-dicyclocarbodiimide (DCC) and 4-dimethylaminopyridine (DMAP) to produce the esters, alkyl (*S*)-2-(6-methoxy-2-naphthyl)propionates, (S)MNP(*n*,*q*). The methoxy group of these esters was demethylated by treatment with BBr_3. The resulting hydroxy group of the alkyl (*S*)-2-(6-hydroxy-2-naphthyl)propionates, (S)HNP(*n*,*q*) was subsequently esterified with 4-(4-alkoxyphenyl)benzoic acid PBA(*p*), using DCC and DMAP, to produce the target compounds (S)HNP (*p*,*n*,*q*). Detailed procedures are described below.

2.2.1. *Alkyl (S)-2-(6-methoxy-2-naphthyl)propionates, (S)MNP(n,q)*

The (*S*)-2-(6-methoxy-2-naphthyl)propionic acid (25 mmol) and required alcohol (27.5 mmol) were dissolved in dry dichloromethane (100 ml). After the addition of DCC (27.5 mmol) and DMAP (2.5 mmol), the solution was stirred at room temperature for five days. The precipitate was filtered and washed with dichloromethane. The filtrate was successively washed with 5% acetic acid, 5% aqueous sodium hydroxide and water, and then dried over anhydrous magnesium sulphate and concentrated in vacuum. The residue was purified by column chromatography over silica gel (70–230 mesh) with dichloromethane as eluant. The isolated ester, in 85–90% yields was identified by ^{1}H NMR spectroscopy and used directly for the follow-up reaction without further purification.

2.2.2. *Alkyl (S)-2-(6-hydroxy-2-naphthyl)propionates, (S)HNP(n,q)*

The alkyl (*S*)-2-(6-methoxy-2-naphthyl)propionate (17.6 mmol) dissolved in dry dichloromethane (66 ml) was mixed with boron tribromide (3.3 ml) at −20°C. The mixture was stirred at −20°C for 5 min, and at 0°C for 40 min. After diluting with dichloromethane (132 ml), the solution was poured into a mixture of saturated ammonium chloride (66 ml) and crushed ice (66 g). The organic layer was separated and washed with brine/ice, dried over anhydrous sodium sulphate and concentrated in vacuum. The residue was purified by column chromatography over silica gel (70–230 mesh) using dichloromethane as eluant. The pure alcohol, in 70–75% yield, was collected after recrystallization from *n*-hexane. Chemical shifts for the typical (S)HNP(0,3) in ^{1}H NMR (400 MHz, $CDCl_3$): δ (ppm) 0.7–1.7 (m, 14H), 1.6 (d, 3H), 3.8–3.81 (q, 1H), 4.8–4.9 (m, 1H), 5.3 (s, 1H), 7.0–7.7 (m, 6H).

2.2.3. *Alkyl (S)-2-{6-[4-(4-alkoxyphenyl)benzoyloxy]-2-naphthyl}propionates, (S)HNP(p,n,q)*

A mixture of 4-(4-alkoxyphenyl)benzoic acid (PBA(*p*), 1.15 mmol), alcohol (S)HNP(*n*,*q*) (1.05 mmol), DCC (1.36 mmol), DMAP (0.13 mmol) and dry tetrahydrofuran (5 ml) was stirred at room temperature for 5 days. The precipitate was filtrated and washed with dichloromethane. The filtrate was successively washed with 5% acetic acid, 5% aqueous sodium hydrogen carbonate and water, then dried over anhydrous sodium sulphate and concentrated in vacuum. The residue was purified by column chromatography over silica gel (70–230 mesh) using dichloromethane as eluant. After purification by recrystallization from absolute ethanol, 60–70% yields of final product were obtained. Chemical shifts for the typical (S)HNP(12,0,3) in ^{1}H NMR (400 MHz, $CDCl_3$): δ (ppm) 0.7–1.8 (m, 37H), 1.6 (d, 3H), 3.8–3.9 (q, 1H), 4.0–4.1 (t, 2H), 4.8–4.9 (m, 1H), 7.1–8.3 (m, 14H). Elemental analysis: calcd C 79.61, H 8.61; found C 80.16, H 8.68%.

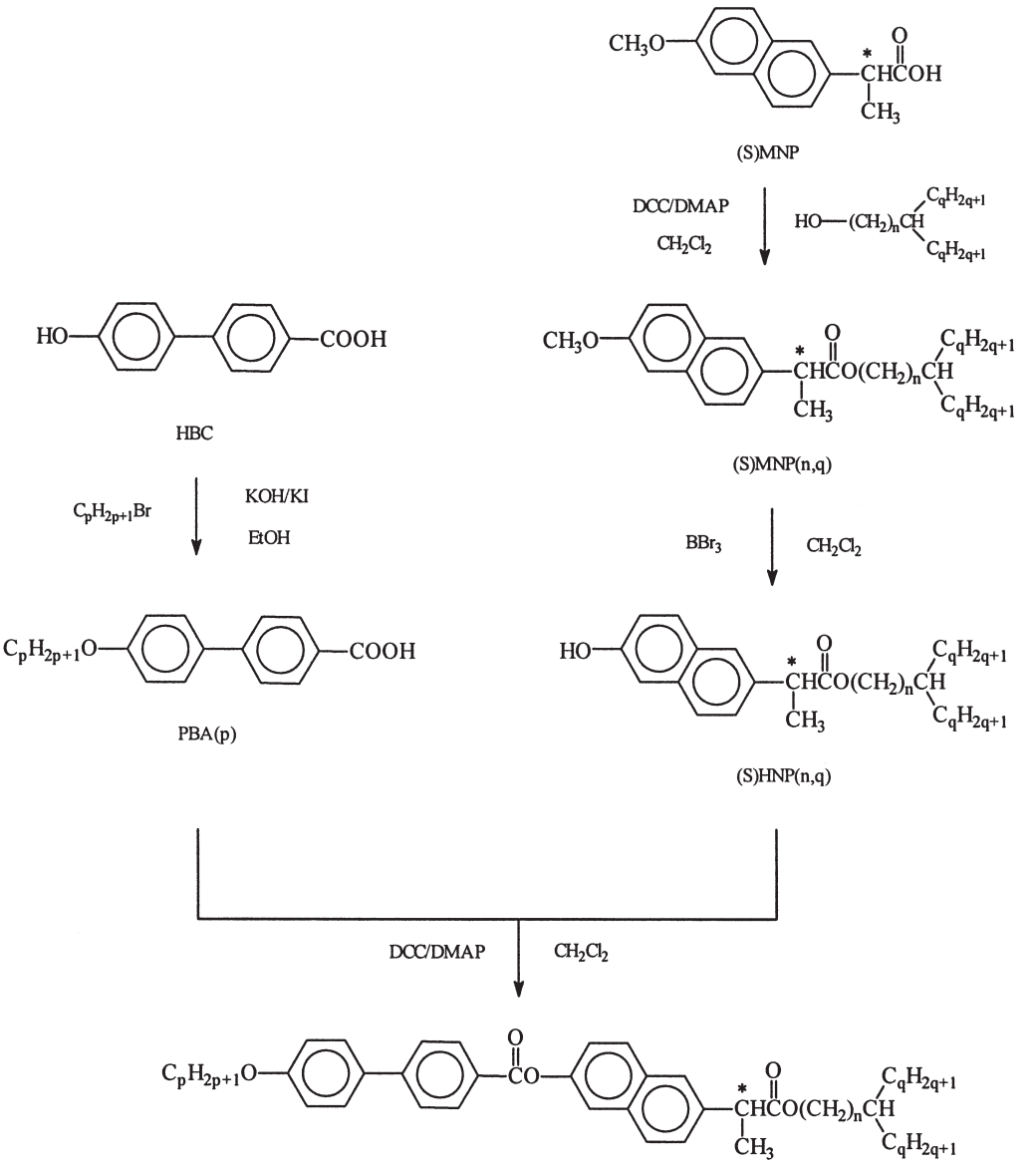

I:(S)HNP(p=8-12,0,2) II:(S)HNP(p=10-12,0,3)

III:(S)HNP(p=8-12,1,2) IV:(S)HNP(p=9-14,0,3)

Scheme. Synthetic procedures for the compounds (*S*)HNP(*p*,*n*,*q*).

3. Results and discussion

3.1. *Mesophase properties*

The mesophases were primarily identified by observing microscopic textures of the compounds sandwiched between two glass plates under crossed polarizers. The N* phase was characterized by the appearance of a scale-like or fan-like texture. As the N* phase changed to the SmA* phase, an intermediary TGB_A^* phase modification was characterized by the appearance of a spiral filament texture [13, 14]. The SmA* phase was identified by of the appearance of homeotropic texture. The SmC_A^* phase appeared as a striated focal conic texture in the thicker sample region, and was further characterized by the schlieren texture with two- and four-brush singularities in the thinner sample region. The mesophases, phase transition temperatures and corresponding transition enthalpies were measured by DSC calorimetry. The results are listed in tables 1–3.

The effect of swallow-tailed groups on the formation

Table 1. Transition temperature and enthalpies of (S)HNP(p,0,3) compounds at 5°C min^{-1} scanning rate.

	T/°C, and ΔH/J g^{-1} (in italics)											
p	I		N*		TGB_A^*		SmA*		Cr		m.p.	
10	•	143.7	•	128.5	•	127.9	•	76.5	•	113.2		
		2.4		*1.0*[a]		[b]		*69.2*		*80.6*		
11	•	134.1	•	122.6	•	121.9	•	66.5	•	89.0		
		2.1		*1.5*[a]		[b]		*60.8*		*64.5*		
12	•	139.8	•	127.0	•	125.2	•	77.3	•	97.1		
		2.2		*1.0*[a]		[b]		*94.6*		*91.8*		

[a]The sum of two transition enthalpies: N*–TGB_A^* and TGB_A^*–SmA*.
[b]The enthalpy was too small to be measured.

of the mesomorphic phases is seen by plotting the phase diagram for compounds (S)HNP (10,n,q; $n=0,1$; $q=2,3$) in figure 1. The SmC_A^* phase was observed in all members of the series (S)HNP(10,n,q) except (S)HNP(10,0,3). These results imply that the swallow-tailed structure may promote the formation of zigzag pairing of the molecules in the smectic phase [9]. Surprisingly none of the compounds of the series (S)HNP(p,0,3) showed the SmC_A^* phase. These compounds have a more steric branching structure than (S)HNP(p,0,2), i.e. propyl versus ethyl, so that a stronger steric effect generated by the swallow-tailed structure is expected. This contradictory result, however, is not clear and cannot be explanated at present. Figure 1 also shows that, on increasing the linking group n from 0 to 1, the higher disordered BP_{II}, N* and TGB_A^* phases disappear.

3.2. *Switching behaviour*

Figure 2 shows the electrical response to the switching of compounds (S)HNP(10,0,2), (S)HNP(10,1,2) and (S)HNP(10,1,3) in 2 μm cells under a triangular wave voltage with field frequency 20 Hz and amplitude 2 $V_{p\text{-}p}$. No switching current peak was observed in the temperature range of SmA* phase. As the temperature cooled in the SmC_A^* phase, two switching current peaks were seen. The relative position of these two peaks was different from results obtained for a normal antiferroelectric phase [15], but similar to our previous report on the antiferroelectric phase of series I [1].

Table 3. Transition temperature and enthalpies of (S)HNP(p,1,3) compounds at 5°C min^{-1} scanning rate.

	T/°C, and ΔH/J g^{-1} (in italics)								
p	I		SmA*		SmC_A*		Cr		m.p.
9	•	114.2	•	97.0	•	78.0	•	94.2	
		4.9		*0.6*		*38.3*		*47.2*	
10	•	111.9	•	98.4	•	69.7	•	87.8	
		5.2		*1.0*		*36.7*		*44.8*	
11	•	108.1	•	98.2	•	64.8	•	86.8	
		6.6		*1.2*		*32.3*		*62.4*	
12	•	107.0	•	99.0	•	61.7	•	86.7	
		4.7		*1.7*		*80.7*		*101.7*	
13	•	105.1	•	98.4	•	61.9	•	87.5	
		7.0		*1.2*		*80.1*		*78.0*	
14	•	104.2	•	98.4	•	67.8	•	91.9	
		4.1		*1.7*		*93.8*		*102.5*	

3.3. *Spontaneous polarization*

Spontaneous polarizations ($\mathbf{P}_S$) values of the compounds were determined in LC cells made of ITO-coated glass whose surface had been treated for parallel alignment with ploymide. Measurements were made after slow cooling to the SmC_A^* temperature range. The $\mathbf{P}_S$ values for each compound depend on temperature and exhibit a maximum. The maximum $\mathbf{P}_S$ values of compounds (S)HNP(p,1,2) were in the

Table 2. Transition temperature and enthalpies of (S)HNP(p,1,2) compounds at 5°C min^{-1} scanning rate.

	T/°C, and ΔH/J g^{-1} (in italics)											
p	I		N*		TGB_A^*		SmA*		SmC_A^*		Cr	m.p.
9	•		—		—	124.1	•	106.7			75.2	97.8
						4.0		*0.5*			*24.1*	*30.5*
10	•		—		—	123.3	•	109.1	•		68.3	96.4
						6.9		*0.9*			*47.9*	*57.4*
11	•	117.7	•	117.5	•	117.4	•	108.3	•		62.0	89.5
		4.8		[a]		[a]		*1.6*			*36.1*	*49.3*
12	•	116.2	•	115.9	•	115.8	•	108.4	•		63.1	84.5
		4.3		[a]		[a]		*1.3*			*36.1*	*49.3*
13	•		—		—	117.3	•	110.9	•		70.6	89.5
						6.3		*1.7*			*67.5*	*70.1*
14	•		—		—	116.6	•	110.7	•		73.8	91.4
						5.1		*1.2*			*60.4*	*63.5*

[a]The enthalpies of N*–TGB_A^* and TGB_A^*–SmA* transitions were added together with that of the I–N* transition.

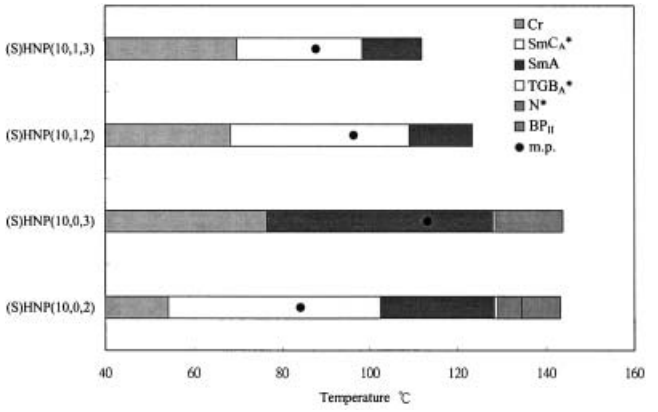

Figure 1. A plot of transition temperature as a function of linking group chain length n and swallow-tailed length q for compounds (S)HNP(10,n,q) on cooling.

range 21–30 nC cm^{-2}, as shown in figure 3; those of compounds (S)HNP(p,1,3) were in the range 15–23 nC cm^{-2}, as shown in figure 4. The first increase in $\mathbf{P}_S$ value with decreasing temperature below T_c can be attributed to decreased thermal motion at the lower temperature. After maximum $\mathbf{P}_S$ is reached, continued lowering of the temperature results in decreasing $\mathbf{P}_S$, which may be due to crystallization.

3.4. *Dielectric properties*

Figure 5 illustrates the temperature dependence of the dielectric constant ε' for the compound (S)HNP(9,1,3) measured at 10 kHz on heating and cooling. The scanning rate is held at 0.2°C min^{-1}. The ε'' values in the SmA* phase are small and increase slightly at the SmA* to SmC$_A^*$ transition. Enhancement of the dielectric constant by the contribution of molecular reorientation is no longer effective in the crystal.

More detailed macro- and micro-molecular motions of molecules in the SmC$_A^*$ phase were investigated by observing the frequency dependence of the dispersion and absorption curves for a sample of compound (S)HNP(10,1,3), as presented in figure 6. The results show that both the real and imaginary parts of the dielectric constant are fairly stable, increase except for frequencies below 1 kHz. The real dielectric constants shows a tendency to diverge (the imaginary loss consistently increases) at higher frequency, 10^5–10^6 Hz. This feature was seen in the empty cell and is presumably due to the polyimide alignment of the film. Thus, here there is no significant occurrence of the relaxation process in the antiferroelectric phase, as seen in MHPOBC [16] and our previous result in series I compounds [1].

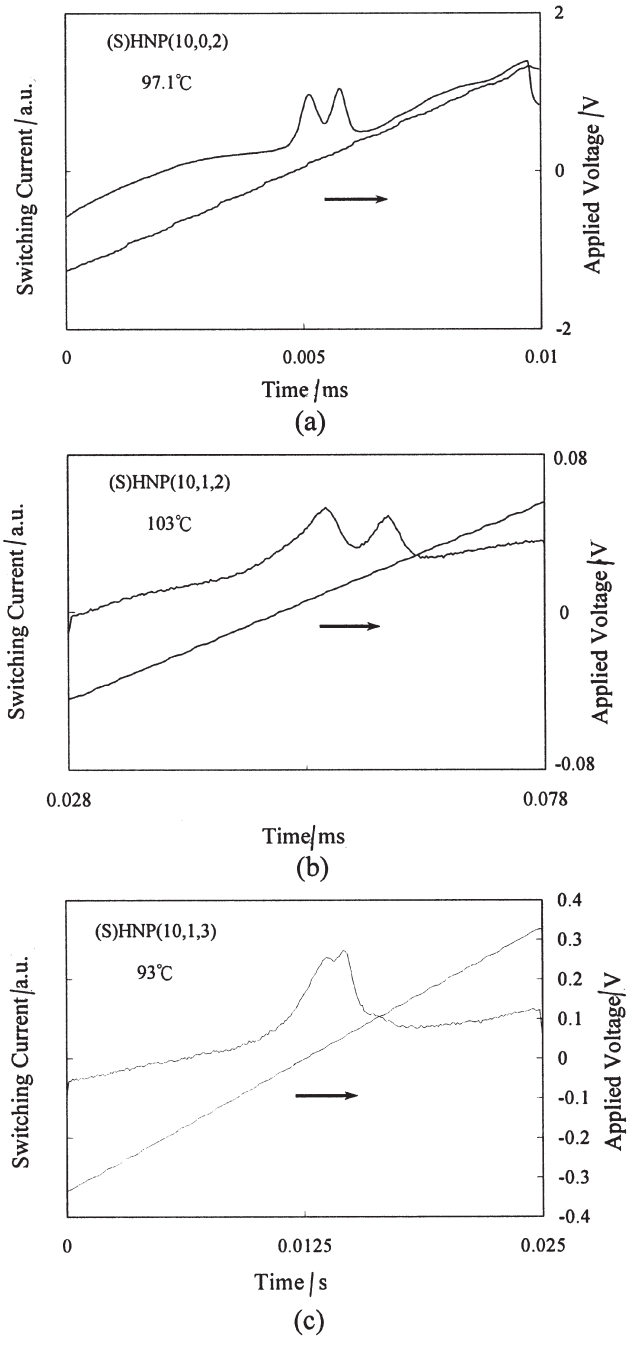

Figure 2. Switching behaviour in the SmC* phase obtained for (S)HNP(10,n,q), with the material confined in a polyimide-coated 2 μm cell. (*a*) $n=0$, $q=2$; (*b*) $n=1$, $q=2$; (*c*) $h=1$, $q=3$.

3.5. *Electro-optical response*

Figure 7 illustrates the responses of the transmittance versus electric field on applying a triangular waveform field measured in the SmC$_A^*$ phase of compounds (S)HNP (10,n,q; $n=0,1$; $q=2,3$). Thresholdless, V-shaped switching was observed in three of these

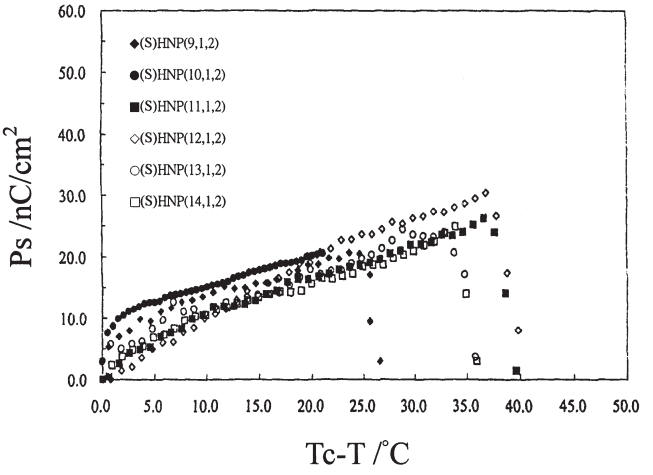

Figure 3. Spontaneous polarization plotted as a function of temperature for (S)HNP(p,1,2; p=9–14). T_c is the SmA*–SmC$_A^*$ transition temperature.

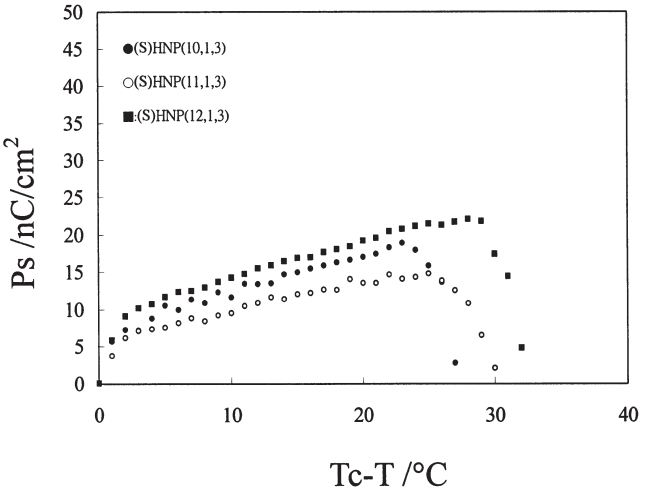

Figure 4. Spontaneous polarization plotted as a function of temperature for (S)HNP(p,1,3; p=10–12). T_c is the SmA*–SmC$_A^*$ transition temperature.

compounds at appropriate temperatures and frequencies. These results imply that variation of the swallow-tailed groups does not significantly change the structural geometry of the SmC$_A^*$ phase of the chiral liquid crystals in surface-stabilized homogenously aligned cells. They also show that V-shaped switching varies with molecular structures, at different temperatures and frequencies.

4. Conclusion

The effect of the variation of swallow-tailed groups on the mesomorphic and electro-optical properties of chiral liquid crystals derived from (*S*)-2-(6-hydroxy-2-naphthyl)propionic acid has been investigated. With the exception of series I(p, 0, 3), these compounds display

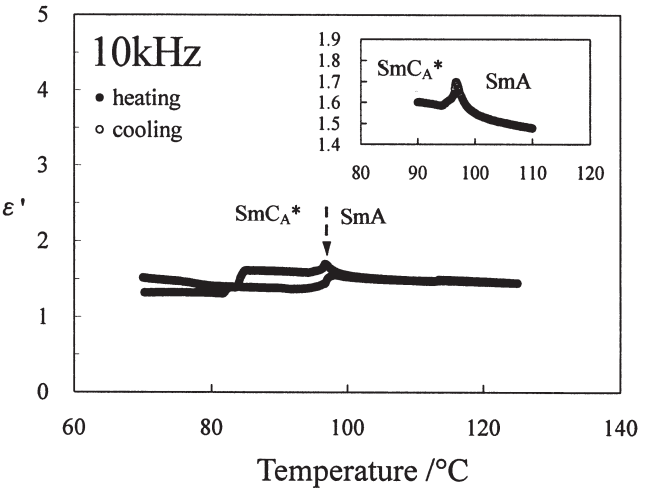

Figure 5. Temperature dependence of the real part of the dielectric constant ε' for (S)HNP(9,1,3).

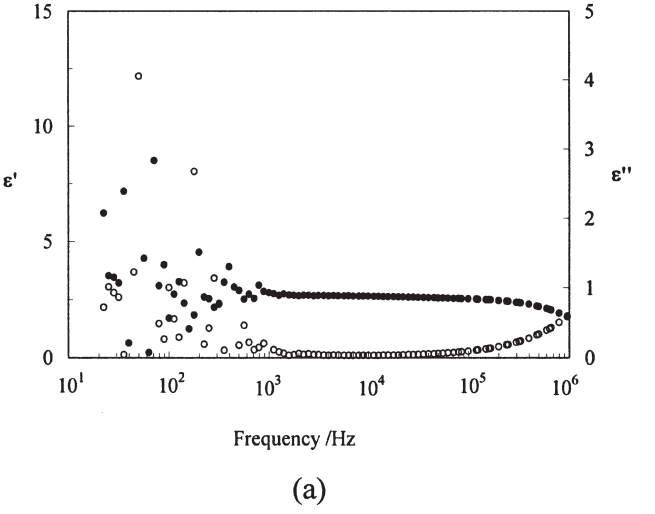

Figure 6. Representative dispersion and absorption curves of compound (S)HNP(10,1,3) plotted as ε' (●) and ε'' (○) versus frequency in (*a*) SmA* phase at 100°C, and (*b*) SmC$_A^*$ phase at 95.0°C.

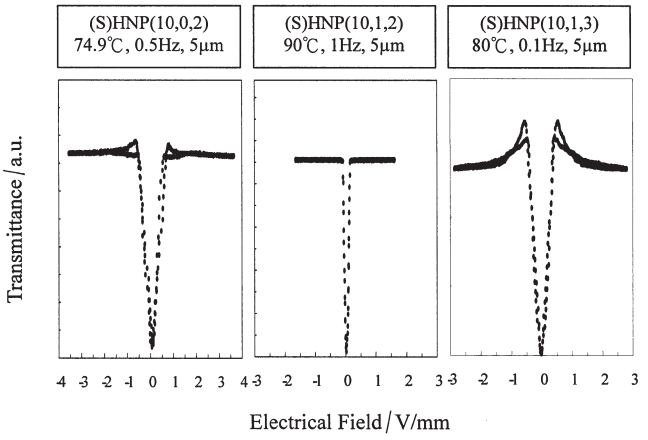

Figure 7. V-shaped switching obtained for (S)HNP(10,0,2), (S)HNP(10,1,2) and (S)HNP(10,1,3) at appropriate temperatures and frequencies.

an antiferroelelctric phase, identified by the observation of switching behaviour and dielectric properties. All the chiral liquid crystals possessing an antiferroelectric phase displayed thresholdless, V-shaped switching, as seen during the measurement of the electro-optical response.

References

[1] Wu, S.-L., and Hsieh, W.-J., 1999, *Chem. Mater.*, **11,** 852.
[2] Wu, S.-L., and Chiang, C. T., 2002, *Liq. Cryst.*, **29,** 39.
[3] Inui, S., Limura, N., Suruki, T., Iwane, H., Miyachi, F., Takanishi, Y., and Fukuda, A., 1996, *J. mater. Chem.*, **6,** 671.
[4] Saishu, T., Takatoh, K., Iida, R., Nagata, H., and Mori, Y., 1996, *SID'96 Dig.*, **28,** 4.
[5] Seomun, S. S., Takanishi, Y., Ishikawa, K., Takezoe, H., and Fukuda, A., 1997, *Jpn. J. appl. Phys.*, **36,** 3586.
[6] Seomun, S. S., Gouda, T., Takanishi, Y., Ishikawa, K., Takezoe, H., and Fukuda, A., 1999, *Liq. Cryst.*, **26,** 151.
[7] Chandani, A. D. L., Cui, Y., Seomun, S. S., Takanishi, Y., Ishikawa, K., and Takezoe, H., 1999, *Liq. Cryst.*, **26,** 167.
[8] Seomum, S. S., Fukuda, T., Fukuda, A., Yoo, J.-G., Panarin, Yu, P., and Vij, J. K., 2000, *J. mater. Chem.*, **10,** 2791.
[9] Nishiyama, I., and Goodby, J. W., 1992, *J. mater. Chem.*, **2,** 1015.
[10] Miyasato, K., Abe, S., Takezoe, H., Fukuda, A., and Kuze, E., 1983, *Jpn. J. appl. Phys.*, **22,** L661.
[11] Wrobrl, S., Hasse, W., Pfeiffer, M., Beresnev, L., and Geelhaar, T., 1992, *Mol. Cryst. liq. Cryst.*, **212,** 335.
[12] Wu, S.-L., Yen, P. C., and Hsieh, W.-J., 1998, *Liq. Cryst.*, **24,** 741.
[13] Wu, S.-L., and Hsieh, W.-J., 1996, *Liq. Cryst.*, **21,** 783.
[14] Kuczynski, W., and Sfegemeyer, H., 1994, *Ber. Bunsenges, phys. Chem.*, **98,** 1322.
[15] Slaney, A. J., Watson, M., and Goodby, J. W., 1995, *J. mater. Chem.*, **5,** 2145.
[16] Suzuki, Y. I., Isozaki, T., Hashimoto, S., Kusumoto, T., Hiyama, T., Takanishi, T., Yakazoe, H., and Fukuda, A., 1996, *J. mater. Chem.*, **6,** 753.